

Spectroscopic ellipsometric characterization of Si/Si_{1-x}Ge_x strained-layer superlattices

H. Yao *, J.A. Woollam

Center for Microelectronic and Optical Materials Research, and Department of Electrical Engineering, University of Nebraska, Lincoln, NE 68588-0511, USA

P.J. Wang, M.J. Tejwani

IBM Semiconductor R&D Center, Hopewell Junction, NY 12533, USA

and

S.A. Alterovitz

Lewis Research Center, National Aeronautics and Space Administration, Cleveland, OH 44135, USA

Received 2 June 1992; accepted for publication 31 July 1992

Spectroscopic ellipsometry (SE) was employed to characterize Si/Si_{1-x}Ge_x strained-layer superlattices. An algorithm was developed, using the available optical constants measured at a number of fixed x values of Ge composition, to compute the dielectric function spectrum of Si_{1-x}Ge_x at an arbitrary x value in the spectral range 1.7 to 5.6 eV. The ellipsometrically determined superlattice thicknesses and alloy compositional fractions were in excellent agreement with results from high-resolution X-ray diffraction studies. The silicon surfaces of the superlattices were subjected to a 9:1 HF cleaning prior to the SE measurements. The HF solution removed silicon oxides on the semiconductor surface, and terminated the Si surface with hydrogen-silicon bonds, which were monitored over a period of several weeks, after the HF cleaning, by SE measurements. An equivalent dielectric layer model was established to describe the hydrogen-terminated Si surface layer. The passivated Si surface remained unchanged for > 2 h, and very little surface oxidation took place even over 3 to 4 days.

1. Introduction

The Si/Si_{1-x}Ge_x strained-layer superlattice (SLS) plays an important role in band-gap engineering and Si-based fast electronic device applications [1,2]. This structure can be grown by low-temperature growth processes, such as molecular beam epitaxy (MBE) or ultrahigh vacuum/chemical vapor deposition (UHV/CVD) [3,4]. In both processes, it is critically important to have tight control on the structural growth parameters such as layer thicknesses, alloy com-

positions and interfacial roughness. In this paper, we report results of spectroscopic ellipsometry (SE) characterization of layer thicknesses, pseudo-alloy-compositions and surface conditions of Si/Si_{1-x}Ge_x SLSs grown by the UHV/CVD technique.

2. Spectroscopic ellipsometry

SE is a non-destructive optical technique. It is extremely sensitive to thickness, alloy composition, and surface and interfacial conditions of the sample structure [5,6]. SE is designed to accu-

* To whom correspondence should be addressed.

rately determine the values of $\tan(\psi)$ and $\cos(\Delta)$, which are the amplitude and projected phase of the complex ratio

$$\rho = R_p/R_s = \tan(\psi) e^{i\Delta}, \quad (1)$$

where R_p and R_s are the complex reflection coefficients of light, measured from the sample, polarized parallel to (p) or perpendicular to (s) the plane of incidence. The results of the SE experimental measurements can be expressed as $\psi(h\nu_i, \Phi_j)$ and $\Delta(h\nu_i, \Phi_j)$ where $h\nu$ is the photon energy and Φ is the external angle of incidence.

In the simplest case, i.e., the sample can be ideally described as a two-phase model (ambient/substrate), R_p and R_s are the Fresnel reflection coefficients. In the case of multilayer-structured samples, a model has to be assumed, and the SE data must be numerically fitted. The values of $\psi^c(h\nu_i, \Phi_j)$ and $\Delta^c(h\nu_i, \Phi_j)$ are calculated as in eq. (1), by an assumed model, for comparison with experimentally measured values. A regression analysis is used to vary the model parameters (e.g., layer thickness or alloy composition) until the calculated and measured values match as closely as possible. This process is done by minimizing the mean square error (MSE) function, defined as:

MSE

$$= \frac{1}{N} \sum_{i,j} \left\{ \left[\tan \psi(h\nu_i, \Phi_j) - \tan \psi^c(h\nu_i, \Phi_j) \right]^2 + \left[\cos \Delta(h\nu_i, \Phi_j) - \cos \Delta^c(h\nu_i, \Phi_j) \right]^2 \right\}. \quad (2)$$

The pseudodielectric function of the sample $\langle \epsilon \rangle$ is obtained from the ellipsometrically measured values of ρ , in a two-phase model (ambient/substrate) [5]:

$$\langle \epsilon \rangle = \langle \epsilon_1 \rangle + i \langle \epsilon_2 \rangle \\ = \epsilon_a \left[\left(\frac{1 - \rho}{1 + \rho} \right)^2 \sin^2 \Phi \tan^2 \Phi + \sin^2 \Phi \right], \quad (3)$$

regardless of the possible existence of surface overlayers or multilayer structures. The ϵ_a in eq. (3) represents the ambient dielectric function (e.g., $\epsilon_a = 1$ in vacuum). To compute the dielectric functions of $\text{Si}_{1-x}\text{Ge}_x$ at an arbitrary x value, we used a group of dielectric functions of bulk

$\text{Si}_{1-x}\text{Ge}_x$ measured at fixed x values [7-9], shown in fig. 1, as the basis of our calculation. From fig. 1, it is noticeable that as the x value increases, each critical point of the energy band, such as E_2 or E_1 , shifts by different amounts. Considering the nature of the non-rigid shifts of the $\langle \epsilon \rangle$ spectrum as the x value changes, an energy-shift model [10] is employed to calculate the $\langle \epsilon \rangle$ spectrum for any x values of Ge. This model has been described in detail in ref. [10]. In this procedure the $\langle \epsilon \rangle$ spectrum is computed for an arbitrary x value of Ge by interpolating between the two known adjacent spectra which are above and below the x value, with weighted averages of the two shifted spectra [10]. For $\text{Si}_{1-x}\text{Ge}_x$, three critical-point transitions are considered: E_2 (~4.37 eV); E_1 (2.1-3.4 eV); $E_{g,\text{ind}}$ (0.76-1.1 eV). The $E_{g,\text{ind}}$ is outside the measuring energy range, but it is needed to interpolate the $\langle \epsilon \rangle$ spectrum at photon energies between $E_{g,\text{ind}}$ and E_1 [10]. Contributions of $E_1 + \Delta_1$ and E_0' to the $\langle \epsilon \rangle$ spectrum are not considered separately here since the positions of these two critical points are very close to that of E_1 . The energy positions of the critical-point transitions E_2 , E_1 , and $E_{g,\text{ind}}$ are given in refs. [11], [7] and [12], respectively:

$$E_2 = 4.372 - 0.069(1 - x) \text{ eV}, \quad (4)$$

$$E_1 = 2.108 + 1.134(1 - x) + 0.153(1 - x)^2 \text{ eV}, \quad (5)$$

$$E_{g,\text{ind}} = 0.8941 + 0.0421(1 - x) \\ + 0.1691(1 - x)^2 \text{ eV} \quad (0 \leq x \leq 0.85), \quad (6)$$

$$E_{g,\text{ind}} = 0.7596 + 1.0860(1 - x) \\ + 0.3306(1 - x)^2 \text{ eV} \quad (0.85 < x \leq 1), \quad (7)$$

where $E_{g,\text{ind}}$ refers to the indirect energy gap of $\text{Si}_{1-x}\text{Ge}_x$ with the X and L minima crossing near $x = 0.85$ [12].

Based on this algorithm, the x value was treated as a parameter in fitting the SE data for the $\text{Si}_{1-x}\text{Ge}_x$ SLSs to find the best-fit pseudo-alloy-composition values x , regardless of the possible influence of strain.

3. Experimental results and discussions

3.1. Sample surface cleaning and passivation

The Si/Si_{1-x}Ge_x SLSs are generally covered with oxides. This oxide surface overlayer has to be modeled for the SE characterization. Si oxide surface is usually modeled as a SiO₂ layer for the SE analysis. However, since the oxide overlayer generally consists of roughness, as well as mixtures of constituents it is necessary to remove the surface oxide and clean the Si surface to obtain the better SE characterization results for Si/Si_{1-x}Ge_x SLSs. Therefore, SE studies of Si surface HF cleaning were carried out prior to the characterization of Si/Si_{1-x}Ge_x SLSs.

p-Type Si wafers (100) of 14–22 Ω·cm resistivity were used to study the effects of HF treatments on Si surfaces covered with native oxide. A piece from the wafer was dipped in 9:1 HF for ~20 s with no rinse. SE measurements were made before and after the HF dip, at a 75° angle

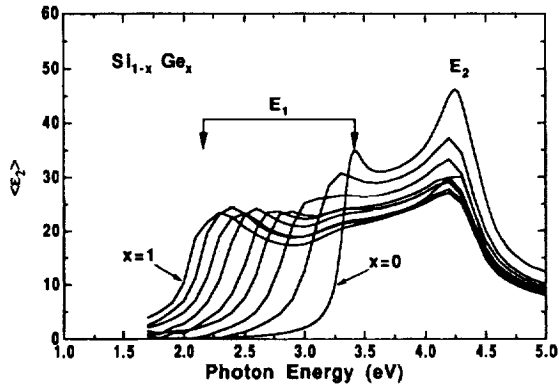


Fig. 1. Imaginary part of the pseudodielectric function $\langle \epsilon_1 \rangle + i\langle \epsilon_2 \rangle$ measured for bulk Si_{1-x}Ge_x, with x decreasing from left to right. The data with $x = 1$ are from ref. [8], those with $x = 0$ are from ref. [9], while the data with other x values: 0.218, 0.389, 0.513, 0.635, 0.75, 0.831 and 0.914 are from ref. [7]. The energy intervals between data points are 0.1 eV for all x , except that for $x = 1$, which is much smaller [8].

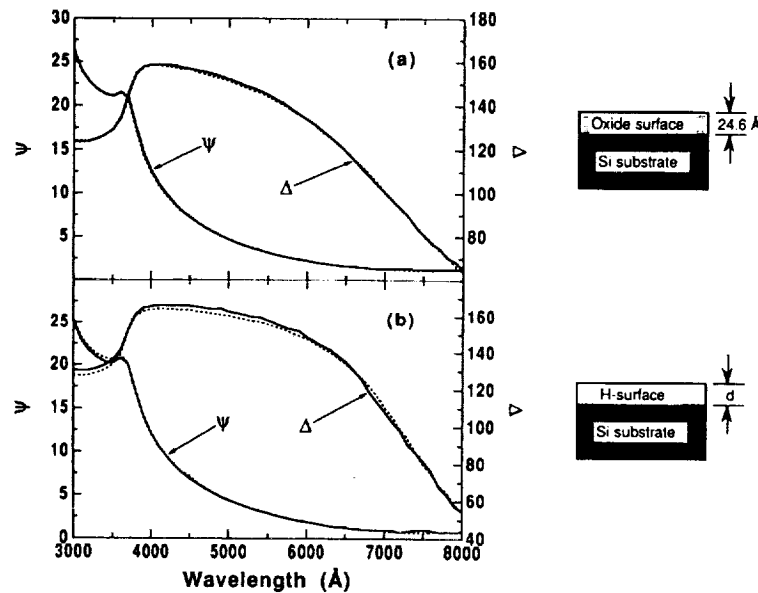


Fig. 2. ψ and Δ values of SE measurements on a Si(100) surface: (a) before and (b) after the HF cleaning. The solid line represents the experimental data, and the dashed line is the best fit of the SE analysis. Assumed models for the SE analysis, in each case, are sketched with the plots.

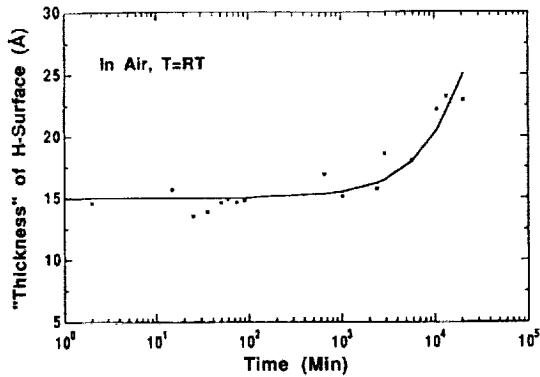


Fig. 3. Changes in effective "thickness" of the hydrogen-terminated Si surface (H-surface) as a function of time, monitored by the SE measurements after the 9:1 HF dip.

of incidence, as shown in figs. 2a and 2b, respectively. As indicated by the SE analysis, this Si sample was initially covered by a native oxide layer with a thickness of 24.6 Å (fig. 2a). After the 9:1 HF dip, the Si oxides were removed and the Si surface was terminated with hydrogen-silicon bonds. This hydrogen-terminated Si surface was modeled as an equivalent dielectric layer described by the optical constants of SiO₂, for the SE analysis shown in fig. 2b. The "thickness" of the hydrogen-terminated Si surface (H-surface), indicated by the SE study, was ~ 14.6 Å

right after the HF cleaning. Notice that the "thickness" referred to here as an "H-surface" was not the actual thickness of the H-surface layer, but the thickness of the modeled equivalent dielectric layer of SiO₂. The value of this "thickness" as measured by SE was used to monitor the changes in the H-surface of Si.

SE measurements were made on this H-surface in air at room temperature (RT) over a period of several weeks, after the HF cleaning. Changes in "thickness" of the H-surface were monitored as a function of time as shown in fig. 3. The figure shows that the hydrogen-terminated Si surface remained unchanged for > 2 h, and very little surface reoxidation took place within 3 to 4 days. Full reoxidation occurred after two weeks. The SE study indicates that the hydrogen termination of the Si surface dangling bonds effectively retards the Si surface oxidation during air exposure.

3.2. SE characterization of the Si/Si_{1-x}Ge_x SLSs

Si/Si_{1-x}Ge_x SLSs with a Ge atomic molar fraction of 8% were grown on Si(100) substrates, at 520°C, by the UFD technique [13]. These Si/Si_{1-x}Ge_x superlattices consist of 20 alternating layers, with a nominal thickness of 200 Å for each layer.

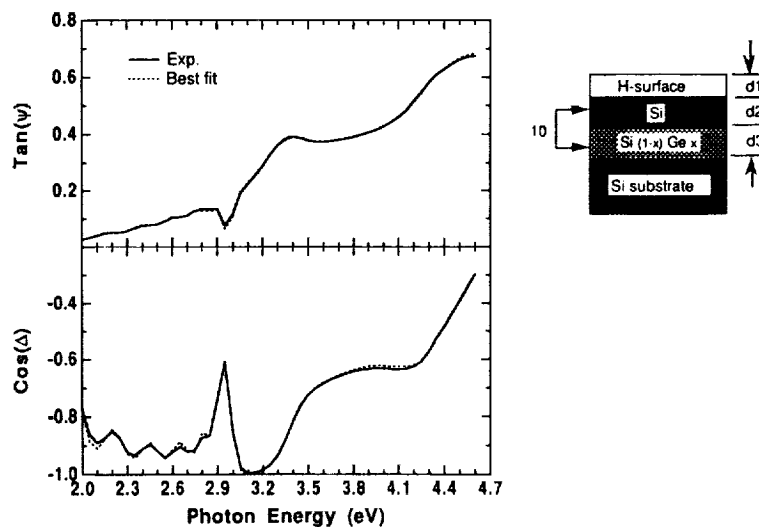


Fig. 4. Results of the SE characterization of the Si/Si_{1-x}Ge_x SLSs. The best fit of the SE analysis is based on the model sketched in this figure, with $d1 = 12.5 \pm 0.2$ Å, $d2 = 216.6 \pm 2.3$ Å, $d3 = 183.9 \pm 2.6$ Å and $x = 0.0610 \pm 0.0008$.

The Si/Si_{1-x}Ge_x SLSs were subjected to a 9:1 HF dip for ~20 s prior to SE characterization. SE measurements were made in air, with an angle of incidence of 75°, in the spectral range 2.0 to 4.6 eV, with an energy interval of 0.05 eV between data points. A sketch of the assumed model for these superlattices, for SE analysis, is shown in fig. 4. In this model, 10 periods of Si/Si_{1-x}Ge_x layers, with thicknesses of d_2/d_3 , were established on a Si substrate. The top hydrogen-terminated surface layer of "thickness" d_1 was modeled as an equivalent dielectric layer of SiO₂, as described in the previous section of this paper. All thicknesses parameters: d_1 , d_2 , d_3 , and the values of pseudo-alloy-composition x were allowed to vary. No interfacial roughness was modeled at this time. Fig. 4 shows the experimental SE data and the best fit from the SE analysis. The best-fit results are: Si 216.6 ± 2.3 Å, Si_{1-x}Ge_x 183.9 ± 2.6 Å and $x = 0.0610 \pm 0.0008$. These results are in excellent agreement with the values of Si 206 ± 5 Å, Si_{1-x}Ge_x 185 ± 5 Å and $x = 0.0825$, from studies of high-resolution double-crystal X-ray diffraction (HRXRD) and cross-sectional transmission electron microscopy (XTEM) by Wang et al. [13]. A MSE value of 3.73×10^{-5} indicates a good fit, and it also reflects high quality of this Si/Si_{1-x}Ge_x SLS with excellent thickness and composition uniformity, grown by the UHV/CVD technique.

Notice that the x value obtained from SE characterization is smaller than that from HRXRD. This is evidence of the strain effects on the Si_{1-x}Ge_x layer. As indicated in ref. [14] and ref. [15], the refractive index of strained Si_{1-x}Ge_x tends to shift towards smaller value, which corresponds to unstrained bulk Si_{1-x}Ge_x with smaller alloy composition value x . It needs to be pointed out that the x value obtained from the HRXRD study considered the strain effects by employing Poisson ratios [13]. The SE measurements seem to magnify the same strain effects on a larger scale. The real reason is not clear.

4. Conclusions

Non-destructive optical SE measurements have been used to characterize the Si/Si_{1-x}Ge_x SLSs

grown by the UHV/CVD technique. Good fits were obtained by SE analysis, with model parameter values consistent with results from HRXRD and XTEM studies. A smaller pseudo-alloy-composition x value is indicative of the strain in the Si_{1-x}Ge_x layer. Ex-situ SE studies of HF cleaning show that the hydrogen termination of the Si surface dangling bonds effectively retards surface reoxidation.

Acknowledgement

This work was partially supported by NASA-Lewis Grant NAG-3-154.

References

- [1] T.P. Pearsall, *Thin Solid Films* 184 (1990) 451.
- [2] S.S. Iyer, G.L. Patton, J.M.C. Stork, B.S. Meyerson and D.L. Harane, *IEEE Trans. Electron Devices* 36 (1989) 2043.
- [3] J.C. Bean, L.C. Feldman, A.T. Fiory, S. Nakahara and J.K. Robinson, *J. Vac. Sci. Technol. A* 2 (1984) 436.
- [4] G.L. Parron, J.H. Comfort, B.S. Meyerson, E.F. Crabbé, G.L. Scilla, E. de Frésart, J.M.C. Stork, J.Y.-C. Sun, D.L. Harame and J.N. Burghartz, *IEEE Electron Device Lett.* 11 (1990) 171.
- [5] R.M.A. Azzam and N.M. Bashara, *Ellipsometry and Polarized Light* (North-Holland, Amsterdam, 1977).
- [6] D.E. Aspnes, in: *Handbook of Optical Constants of Solids*, Ed. E.D. Palik (Academic Press, New York, 1985) p. 89.
- [7] J. Humlíček, M. Garriga, M.I. Alonso and M. Cardona, *J. Appl. Phys.* 65 (1989) 2827.
- [8] D.E. Aspnes and A.A. Studna, *Phys. Rev. B* 27 (1983) 985.
- [9] G.E. Jellison, Jr., *Opt. Mater.* 1 (1992) 41.
- [10] P.G. Snyder, J.A. Woollam, S.A. Alterovitz and B. Johs, *J. Appl. Phys.* 68 (1990) 5925.
- [11] J. Humlíček, F. Lukeš and E. Schmidt, *Solid State Commun.* 42 (1983) 387.
- [12] S. Krishnamurthy, A. Sher and A. Chen, *Appl. Phys. Lett.* 47 (1985) 160.
- [13] P.J. Wang, M.S. Goorsky, B.S. Meyerson, F.K. LeGoues and M.J. Tejwani, *Appl. Phys. Lett.* 59 (1991) 814.
- [14] G.M.W. Kroesen, G.S. Oehrlein, E. de Frésart and G.J. Scilla, *Appl. Phys. Lett.* 60 (1992) 1351.
- [15] M. Racanelli, C.I. Drowley, N.D. Theodore, R.B. Gregory, H.G. Tompkins and D.J. Meyer, *Appl. Phys. Lett.* 60 (1992) 2225.



DEVELOPMENT OF $\text{Si}_{1-x}\text{Ge}_x$ TECHNOLOGY FOR MICROWAVE SENSING APPLICATIONS

Rafael A. Mena, Susan R. Taub, and Samuel A. Alterovitz
National Aeronautics and Space Administration
Lewis Research Center
Cleveland, Ohio 44135

Paul E. Young
University of Toledo
Toledo, Ohio 43606

Rainee N. Simons
Sverdrup Technology, Inc.
Lewis Research Center Group
Brook Park, Ohio 44142

and

David Rosenfeld^{*}
National Aeronautics and Space Administration
Lewis Research Center
Cleveland, Ohio 44135

Abstract

This report discusses the progress for the first year of the work done under the Director's Discretionary Fund (DDF) research project entitled, "Development of $\text{Si}_{1-x}\text{Ge}_x$ Technology for Microwave Sensing Applications". This project includes basic material characterization studies of silicon-germanium (SiGe), device processing on both silicon (Si) and SiGe substrates, and microwave characterization of transmission lines on silicon substrates. The material characterization studies consisted of ellipsometric and magneto-transport measurements and theoretical calculations of the SiGe band-structure. The device fabrication efforts consisted of establishing SiGe device processing capabilities in the Lewis cleanroom. The characterization of microwave transmission lines included studying the losses of various Coplanar transmission lines and the development of novel transitions on silicon. This report discusses, individually, each part of the project and presents the findings for each. Future directions are also discussed.

Introduction

Silicon technology has never been considered viable for microwave applications because of its lack of high frequency active devices and the extremely high dielectric loss associated with silicon substrates. But silicon technology provides many benefits for microwave applications. Among them are: integration with digital circuitry, mature, well-defined processing procedures and low cost. Recently, a new material, SiGe (silicon-germanium), has emerged that can produce high frequency active devices in a silicon based technology. Using SiGe it is possible to fabricate devices with a two-dimensional electron gas (2DEG). This type of structure has advantages in terms of frequency of operation, noise

^{*}National Research Council—NASA Research Associate at Lewis Research Center.

performance and performance improvements at low temperatures. To reduce the dielectric losses associated with silicon substrates, it has been theorized that silicon of sufficiently high resistivity must be used [1].

The purpose of this research project is the development and characterization of microwave devices, both passive and active, using newly-developed SiGe technology at frequencies required for microwave sensing applications. This effort has included basic material studies of SiGe, the development of high electron mobility transistor (HEMT) devices and characterization of microwave transmission lines on high resistivity silicon.

In order to carry out the goals of the program, a working group was established consisting of several members of the Solid State Technology Branch. In this manner, people representing different areas of expertise were brought together. Material, device and circuit experts were all present from the onset of the program. This allowed all areas to be taken into account during planning. Since Lewis does not have the facilities necessary to grow SiGe material, industry and universities were relied upon for the preparation of the SiGe samples. Collaboration was established with UCLA, University of Michigan, Cornell University, Hughes and Spire Corporation. These universities and companies have provided HEMT structures, both n-type and p-type, as well as single strained layers for material characterization studies and device fabrication. It was important to find several sources for material preparation because SiGe technology is in its infancy and there are many uncertainties involved in its growth.

The program consisted of three different areas of research while maintaining a common objective among the members of the working group. The research areas consisted of: basic material studies, device processing and, microwave characterization studies. In a relatively short period of time, many of the goals of this three year program have been accomplished. This report describes the progress for the first year and discuss future directions.

Basic Material Characterization Studies

Theoretical Study

The objective of the theoretical study was to gain a better understanding of the relationships between the physical parameters of the layers in a SiGe structure (composition, grading, doping, and mobility), and the device performance parameters (unity current gain frequency and maximum oscillation frequency). The knowledge of these relationships is required in order to design an optimum structure for high-speed, low-temperature applications.

The procedure used to analyze these relationships was to calculate the band structure of the layers and then calculate the performance which results from that band structure. Because of the complexity of the mathematical problem associated with these calculations, as well as some other non-trivial aspects, a collaboration with the Computational Material Lab at NASA Lewis was established. This lab specializes in complicated matter-related numerical calculations. With the help of the Computational Material Lab, the creation of a sophisticated computer code that solves the Poisson equations and calculates the band structure and the currents of SiGe was recently completed. The I-V characteristics of some simple SiGe structures have been calculated and plotted.

Ellipsometry Work

SiGe material samples were obtained from Spire, UCLA, University of Michigan and Hughes. They included: single SiGe strained layers on silicon, Supperlattice SiGe-silicon, and n- and p-type HEMT structures. Only the results obtained for the n-type MODFET

structures provided by UCLA and Spire will be discussed here. These samples consisted of a strained silicon layer for improved carrier confinement and are labeled as follows: 1) Spire D-5983, 2) UCLA MT-115. The results of Ellipsometric characterization of these samples is shown in Table 1.

Ellipsometric characterization of the samples included three steps: measurement, modeling and linear regression analysis. In the first step, the change in the state of polarization of a monochromatic light, that is reflected from the sample, is measured. This change in polarization is represented quantitatively using the ellipsometric parameters φ and Δ . The measurement was repeated for approximately 50 wavelengths and several angles of incidence. Thus, a large number of experimental φ and Δ are estimated. The sample is modeled using the estimated composition and thickness of all the layers in the sample. In the present case, the model consisted of the nominal compositions and thicknesses of all layers as supplied by the sample grower. They are denoted "nominal" in Table 1. The last step included a linear regression least square fit of all the experimental φ and Δ to the theoretically evaluated φ and Δ associated with the model. The minimization parameters were the composition of the SiGe layer and all layer thicknesses. The theoretical φ and Δ associated with the model were calculated using standard Fresnel reflection equations, and published dielectric functions of all material constituents.

The calculation was done using unpublished calibration functions supplied by J. Jellison from Oak Ridge National Laboratories. The dielectric functions supplied by Jellison were interpolated using a numerical algorithm. These functions were measured on relaxed layers of SiGe on silicon. Measurements were done at 3-5 angles of incidence in the range 3000-7500Å using 100Å steps. The wavelength (λ) range was limited so that the light did not penetrate the SiGe buffer layer into the silicon substrates. The concentration 'x' in the SiGe top layer and the "substrate" was assumed to be the same and no roughness was assumed. Graphs of the experimental DELTA (Δ) and PSI (φ) verses model calculations are shown in Fig. 1a,1b,1c,1d.

The reason the strained silicon layers have a lower thickness than the nominal value is probably due to the fact that the unstrained calibration function was used. This was done, because, as of now, no strained silicon calibration function exists. The results for D-5983 indicate that it was a poor quality sample, because the thickness and composition were very different from the nominal values. In comparison, sample UCLA MT-115 appeared much better.

Magneto-Transport Measurements

The most important characteristic of a HEMT structure is the two dimensional nature of its transport properties. This characteristic enables very high speed, low noise performance in active semiconductor devices. SiGe n-type structures have been shown to have very high mobilities, as high as $10^5 \text{ cm}^2/\text{V}\cdot\text{s}$ at low temperatures, which indicate that this is an excellent structure for microwave applications. It is very difficult however, to obtain two dimensionality in this structure since the conduction band discontinuity between silicon and SiGe is very small. This makes it difficult to achieve quantization of the carriers at the interface of the two layers. Two dimensional transport has only been obtained in the n-type structures by growing a strained silicon layer on top of a fully relaxed SiGe layer. The strain pushes down on the conduction band of the higher bandgap silicon layer, relative to the SiGe conduction band and thus makes possible the quantization. High quality strained layers are very difficult to grow as a result of misfit dislocations that arise from the lattice mismatch growth of the epitaxial layers. Because of this, the transport characteristics of the received samples had to be characterized.

N-type SiGe structures have been received from Spire, UCLA, University of Michigan and AT&T. Hall and Shubnikov-de Haas measurements were carried out using a 1.4 Tesla magnet at temperatures from room temperature down to 1.4K. Two dimensional transport was not detected in any of the structures. Therefore, transport must have occurred in either the bulk of the silicon or SiGe layers; as evident by the large carrier freeze-out at lower temperatures and the large magneto-resistance observed in the samples. Carrier freeze-out in a two dimensional electron gas (2DEG) leads to only a small decrease in the carrier concentration. In the structures examined here, the carrier concentration decreased by orders of magnitude as the temperature decreased. For example, the Spire sample went from a concentration of $7.22 \cdot 10^{12}/\text{cm}^2$ at 300K to a concentration of $1.5 \cdot 10^7/\text{cm}^2$ at 22K. This type of behavior was typical of all the samples. The freeze-out temperature of the samples varied between 20K and 50K.

Two dimensional transport was detected in the p-type structure provided by Hughes. As compared with the n-type structures, two dimensional transport in p-type structures is easier to achieve. This is due to the larger band discontinuity in the valance band of the silicon and SiGe layers. Doping the layers is also more simple for p-type structures and thus more accurately controlled. The mobility increased with decreasing temperature due to a reduction in phonon scattering effects. The drop in concentration is consistent with carrier freeze-out in the quantized states.

These results have been provided to the material suppliers and has led to modifications in their growth process. UCLA is attempting to lower the concentration of the capping layer (used for contact purposes), in order to reduce the band bending that occurs at such high concentrations. At Lewis, there is an attempt being made to etch away some of the doped layers, with the intent of reducing the band bending and increasing the energy discontinuity.

Device Processing

Much like the GaAs based high electron mobility transistor (HEMT) technology, SiGe HEMT technology offers the ability to fabricate active devices with low noise and high speed performance. SiGe HEMT technology has the added advantage of silicon's native oxide for metal-oxide-semiconductor (MOS) devices. The advantages of the MOS structure is the decrease in gate leakage and the improvement in device stability as compared to Schottky barrier structures.

To achieve device fabrication capability at Lewis, initial design and fabrication development projects were conducted. The intention of these projects was to develop processing techniques necessary for the fabrication of devices. Etching of SiGe materials was the first processing step required to achieve device patterning and was also needed to expose material layers for further device fabrication. Experiments were conducted to characterize etch rates for SiGe materials.

To achieve optimum device operation, low resistance contacts are critical. Therefore, development of a contact structure has been investigated. The focus of this research has been on antimony based contacts and ion implantation of the contact regions. Antimony based contacts studies were conducted using metal type, metal thickness, alloy temperature and alloy time as variables to determine optimum contact resistance. Figure 2 illustrates some of the results used to determine the proper contact procedure for SiGe devices. The figure shows the effect of various alloying temperatures on the series resistance on contacts of various composition. Studies were also conducted by ion implanting phosphorus ions into the material to create contact regions suitable for aluminum based contacts. Because a heterostructure is being used, contact to the 2DEG is required to provide ohmic contact to the

carriers. Ion implantation is used because it creates a conduction path from the upper contact region to the channel.

In order to fabricate MOS type devices, an oxide is necessary. Oxide characteristics were investigated by examining C-V and I-V measurements. To insure that no interdiffusion of the germanium or donor impurity into the silicon channel layer occurred, a low temperature plasma enhanced chemical vapor deposition (PECVD) technique was used. A characteristic C-V curve is shown in Figure 3. It illustrates the ability to invert the channel region under the oxide and good saturation in the accumulation region. Analysis of the interface state density shows a minimum of $3 \cdot 10^{10}$ states/cm² using the Terman method. The capacitor turn on voltage can be adjusted via processing techniques to plus or minus 5 volts to compensate for charge screening at the inversion layer of the oxide, thus achieving an effective modulation of the 2D carriers.

This work was then used to fabricate a preliminary transistor design. Ion implantation was used in fabricating the contacts. A cross section of the device structure and a finished device are shown in Figures 4 and 5, respectively. Initial evaluation of the device indicated a suppressed transconductance. This was most likely caused by poor material. Contact and oxide resistivities were acceptable but the modulated carrier concentration was extremely low. This resulted in poor device performance. Future device fabrication will be conducted on improved materials. At that time, rf performance as a function of temperature will be measured.

Microwave Transmission Line Studies

To make microwave applications on silicon possible, silicon with sufficiently high resistivity must be used to minimize the dielectric loss. The aim of this segment of the DDF is to investigate the effective dielectric constant (ϵ_{eff}) and attenuation of various transmission lines on silicon as a function of resistivity. We investigated Coplanar Waveguide (CPW), Coplanar slotline and Coplanar stripline structures.

The CPW structures were evaluated theoretically and experimentally. The theoretical analysis was based on the expressions in [2] for ϵ_{eff} and attenuation. The data for attenuation is shown in Figure 6. These calculations are for 2 μm gold lines on 203 μm thick silicon wafers. In this figure, dielectric loss is shown as a function of silicon resistivity for CPW lines of various geometries. Conductor loss is not shown because it is independent of the substrate. It can be seen that the loss is independent of CPW geometry. Losses for wafers of low resistivities are extremely high, but they decrease quickly with increasing resistivity. At a resistivity of 3000 ohm-cm, the dielectric loss is approximately 0.1 dB/cm, which is acceptable. The effective dielectric constant, ϵ_{eff} was calculated to be 6.06 for a CPW line, $S=100\mu\text{m}$, $W=50\mu\text{m}$. Experimentally, the ϵ_{eff} and attenuation were obtained by deembedding these parameters from measurements of several CPW lines on silicon using software from NIST. The theoretical results showed that if silicon with resistivity of 3000 ohm-cm was used, the losses would be comparable with those of the same CPW lines on GaAs (Gallium Arsenide). CPW lines of varying geometries were fabricated on silicon with resistivity of 3000-4000 ohm-cm. The values obtained for ϵ_{eff} and attenuation are shown in Figures 7 and 8 respectively. For the data shown, $S=50\mu\text{m}$, $W=25\mu\text{m}$, wafer thickness = 300 μm and the gold thickness is approximately 1.7 μm . Although no exact theoretical calculations have been done for these particular lines, the measured values are in the expected range. The noise in both curves around 34 GHz was found to be due to cable resonances.

The Coplanar Stripline and slotline structures were evaluated experimentally using resonator methods (since the NIST deembedding software only works for CPW structures).

These methods were first validated on a much cheaper and easier to handle microwave material - RT Duroid 5810.5. This material has a dielectric constant (ϵ_r) of 10.5 (silicon has one of 11.7) and a loss tangent of 0.0028. The slotline structure was evaluated using a ring resonator that produces multiple resonances allowing many frequencies to be evaluated. The Coplanar stripline was evaluated using a series gap coupled straight resonator. The results, experimental and theoretical are summarized in Table 2.

In order to test the slotline, a transition from a CPW to the slotline was developed, since CPW lines can be wafer-probed and slotlines cannot. Two different transitions were developed. The first makes use of a finite ground plane coplanar waveguide (FCPW) which is electromagnetically coupled to a slotline. The second makes use of a conventional CPW which is coupled to the slotline with an airbridge. The average measured performance of both transitions (measured using two back-to-back transitions with about 0.8" of slotline in between) on Duroid substrate gave a maximum insertion loss of -1.5 dB and return loss of better than -10 dB over the frequency range of 3 to 8 GHz.

Second Year Objectives

The efforts of the second year will focus on continuing the collaboration that has been established with the various universities and corporations. The team at Lewis will work more closely with these organizations in the growth and preparation of the SiGe material structures. Results obtained from ellipsometric and magneto-transport measurements carried out at Lewis, will be used to calibrate the growth process and to further understand the material characteristics of various SiGe structures.

The device processing efforts established during this first year will also be continued. The focus will be on improving the performance of the MOS transistor fabricated here at Lewis. Higher quality material, as well as a more complete understanding of processing procedures, will help make this possible. Once suitable material has been obtained and a device fabricated, the rf performance as a function of temperature, will be characterized using an custom variable temperature cryostat. Dramatic improvement in the rf performance is expected at the lower temperatures because of the increase in the mobility of the majority carriers.

Microwave studies will continue and expand to include the development of passive microwave applications on silicon. This will include determining loss as a function of resistivity for CPW lines and the continuing development of slotline and CPW striplines on silicon. Applications such as: phase shifters and antennas will be developed. This is in preparation for the third year effort which will involve combining the microwave passive with the active devices to form truly integrated SiGe circuits.

Conclusion

We have been successful in establishing collaboration with universities and industry for the growth of the SiGe structures. Results obtained from ellipsometric and magneto-transport measurements, carried out at Lewis, were used in the calibration of the growth process as well as to further understand the material characteristics of SiGe. Also, theoretical calculations of the band structure and I-V characteristics of some simple structures, were carried out using a code that was developed at Lewis. We have also been successful in establishing a SiGe device processing capability in the Lewis cleanroom. Preliminary results have been obtained for a MOS transistor device. Finally, we have favorably ascertained the feasibility of silicon as a substrate for microwave applications. Theoretical calculations have shown that transmission line losses are similar to those of GaAs if the substrate resistivity is

kept above a certain value. We have also evaluated experimentally Coplanar Stripline and slotline structures using resonator methods.

References

- [1] Rosen, A., et al. "Silicon as a Millimeter-wave Monolithically Integrated Substrate-a New Look", RCA Rev., 1981, 42, pp. 633-660.
- [2] Gupta, K.C., R. Garg, I.J. Bahl. Microstrip Lines and Slotlines. Artech House, Inc. 1979. pp. 285-287 and 275-276.

a) Layer	Nominal	Ellipsometry
SiO ₂	-----	6±1
Silicon	200 angstroms	113±3
Si _{1-x} Ge _x	500 angstroms	498±6, x=0.233±0.011
Silicon	500 angstroms, x=0.30	114±11
Si _{1-x} Ge _x	x=0.30	x=0.233±0.011
	Substrate	

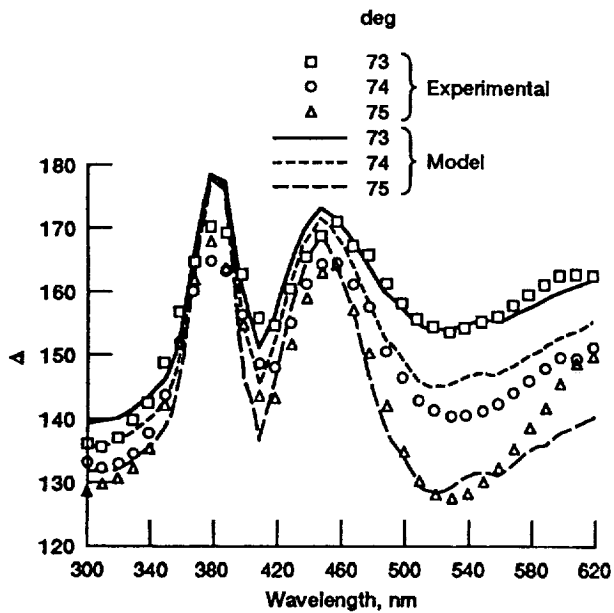
b) Layer	Nominal	Ellipsometry
SiO ₂	-----	26±1
Silicon	400 angstroms, x=0.35	428±3
Si _{1-x} Ge _x	150 angstroms	0.338±0.004
Silicon	x=0.35	135±4
Si _{1-x} Ge _x	Substrate	0.338±0.004

Table 1: Results of ellipsometric study of SiGe structures. a) D-5983, mean square error= 7×10^{-4} b) UCLA MT-115, $\lambda \leq 6400$ angstroms mean square error= 2×10^{-3}

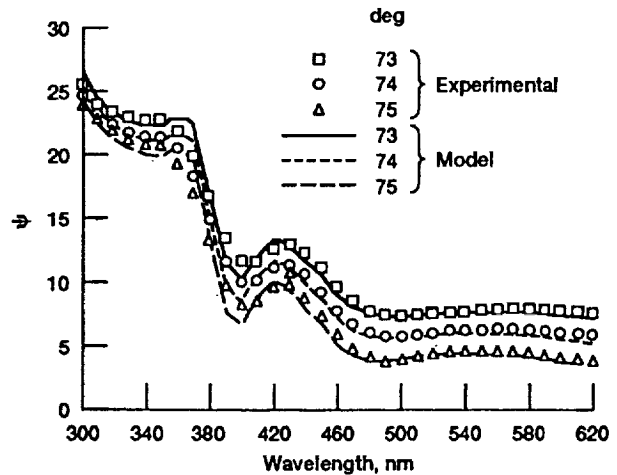
a) Slotline			
Frequency (GHz)	Measured ϵ_{eff}	Computed ϵ_{eff}	Measured Attenuation
25.4	4.1918	4.2093	0.4374
18.8	4.0415	3.9413	0.3471
12.1	3.7996	3.5932	0.2189

b) Coplanar Stripline				
Frequency (GHz)	Measured ϵ_{eff}	Computed ϵ_{eff}	Measured Attenuation	Computed Attenuation
6.2	*	3.9872	0.139	0.111
11.0	*	4.7451	0.158	0.150

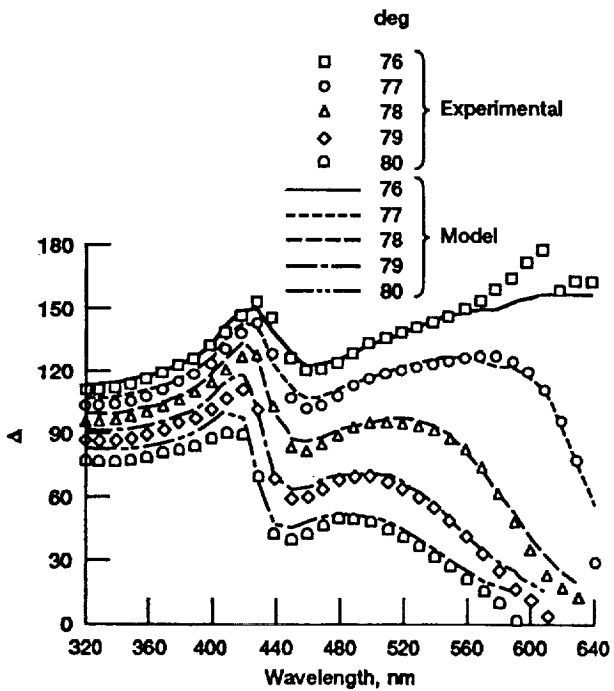
Table 2: Characteristics of ring resonators on high resistivity silicon a) Slotline b) Coplanar Stripline



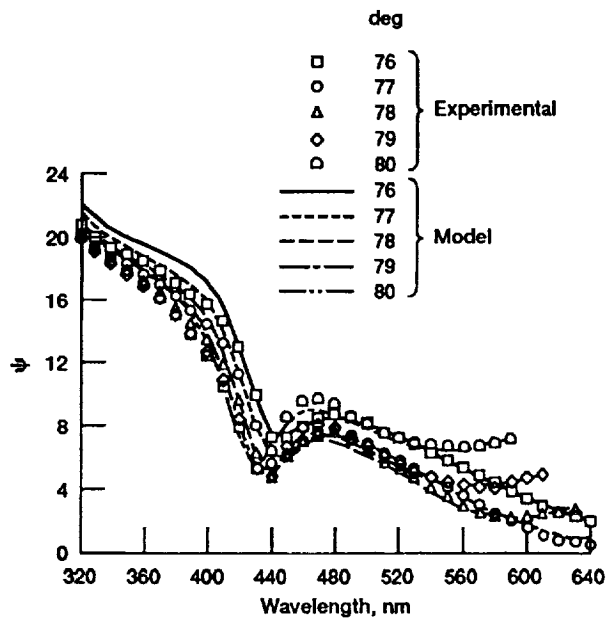
(a) Spire Corporation D-5983; measurement versus model.



(b) Spire Corporation D-5983; measurement versus model.



(c) UCLA MT-115; measurement versus model.



(d) UCLA MT-115; measurement versus model.

Figure 1.—Ellipsometry data.

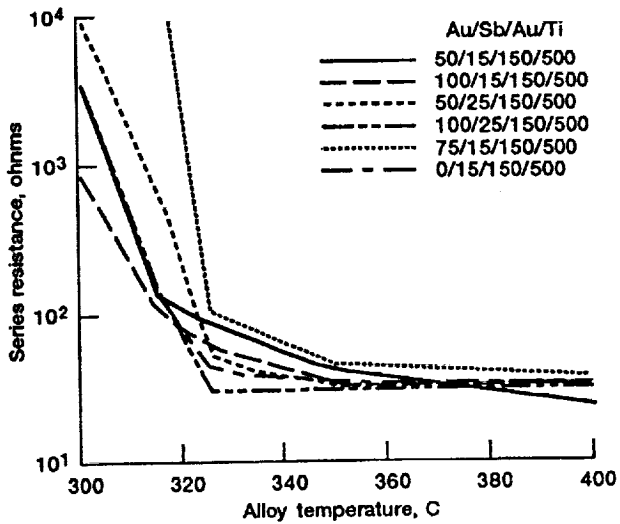


Figure 2.—Series resistance as a function of temperature for various Au/Sb/Au/Ti contacts on silicon.

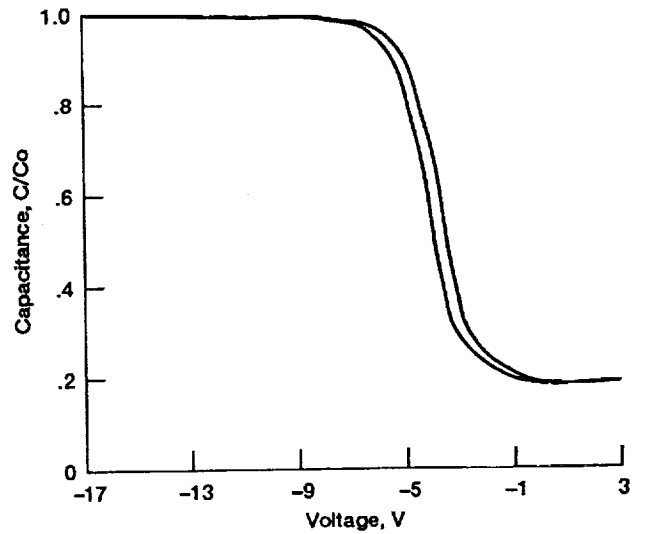


Figure 3.—C-V curve of oxide on SiGe.

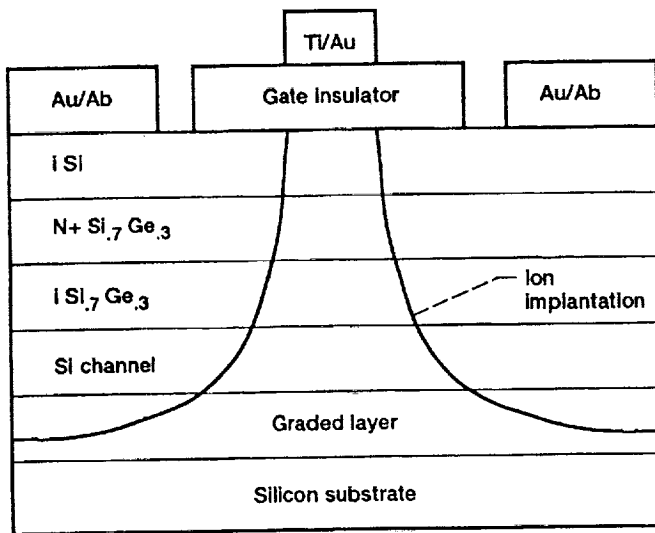


Figure 4.—Self gate aligned SiGe MOS-MODFET-device structure.

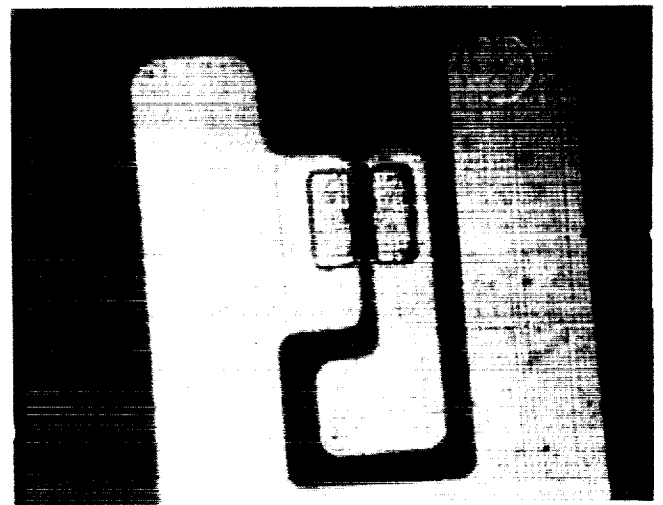


Figure 5.—Self gate aligned SiGe MOS-MODFET finished device.

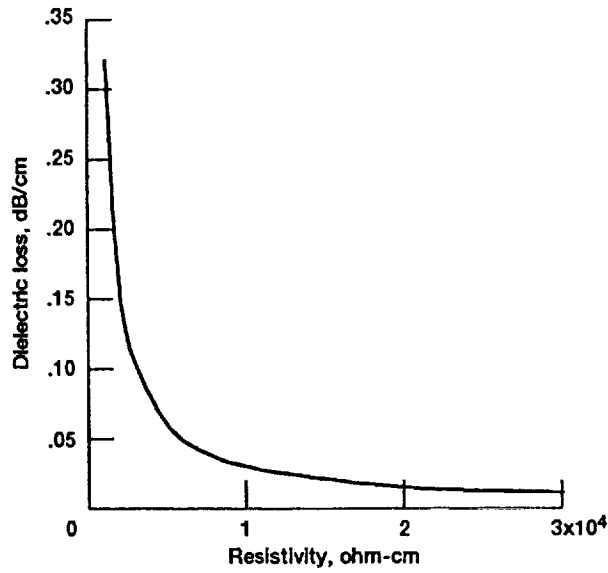


Figure 6.—Theoretical dielectric losses of CPW lines on silicon as a function of resistivity.

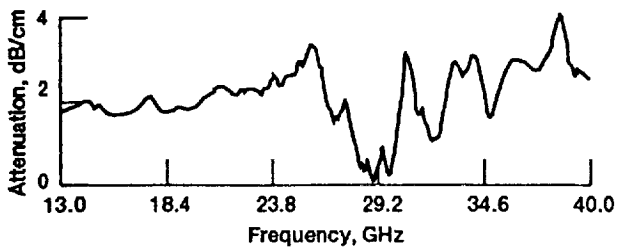


Figure 7.—Measured attenuation.

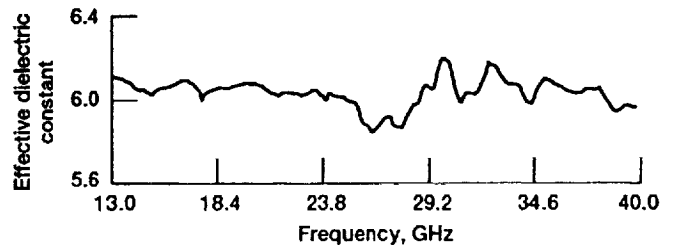


Figure 8.—Measured effective dielectric constant.

